CONTRIBUTION TO EXTRUDATE SWELL FROM THE VELOCITY FACTOR IN NON-ISOTHERMAL EXTRUSION

B. Phuoc HUYNH

Faculty of Engineering, University of Technology, Sydney, NSW 2007, AUSTRALIA

ABSTRACT

The process of non-isothermal extrusion of Newtonian fluids through circular and annular dies is considered. Specifically, the contribution to extrudate swell from the velocity distribution at die exit is examined, using a finite element method. It is found that when different temperatures are imposed on the die walls, this velocity distribution can account for a significant, but still minor in general, portion of the total thickness swell and deflection (in annular extrusion) of the extrudate. When die walls have the same temperatures, however, the contribution from velocity is much further reduced and becomes insignificant in most cases. This leaves viscosity variation due to temperature change confirmed as the dominant factor in affecting the extrudate's swelling behaviour.

INTRODUCTION

This work is concerned with a numerical study of the contribution to extrudate swell from the velocity factor in non-isothermal extrusion. The other factor, due to viscosity change as a result of temperature variation, can then be estimated by deduction.

Extrusion is an important manufacturing process, and extruded products abound. Extrusion through annular dies in particular has application in the manufacturing of pipes and is closely related to processes like film blowing and wire coating. In studying the extrusion process, the material to be extruded is often modelled as a viscous fluid. However, it is known that when such a fluid is extruded through a die, in general the extrudate does not have the same size as the die orifice. The amount of change in extrudate size, known as swelling, is of significant theoretical and practical interest, given the nature of the flow phenomenon involved and the accurate dimensions required of many of the extruded products. It is therefore not surprising that extrudate swell has been among the parameters of primary interest in many investigations; see, for example, Phuoc and Tanner (1980), Vlachopoulos (1981), Mitsoulis (1986), Seo (1990), Ahn and Ryan (1992), Huynh (1998a), and the references therein.

Temperature has been seen to be among the many factors affecting extrudate swell (Phuoc and Tanner, 1980; Vlachopoulos, 1981; Seo, 1990; Ahn and Ryan, 1992; Huynh, 1998a). In particular, it has been shown recently (Huynh,1998a, 1998b) that large variations of swelling of the extrudate can result when the extrusion flow is non-isothermal, especially when die walls are prescribed with temperatures that are significantly different from the fluid's bulk temperature. However, since temperature affects the fluid's properties, and most importantly its viscosity, and this in turn affects the flow field, it is not clear as to the contribution to swelling from each factor, viscosity change and velocity distribution, because both have been known to influence the swelling phenomenon: the viscosity influence as per a theory due to Tanner (Tanner, 1980; Huynh, 1983), whereas extrudate swell also occurs in isothermal situation and thus is due to the re-arrangement of the velocity field (Karagiannis et al., 1989).

In an effort to provide further understanding of the extrudate swell phenomenon, a main aim of this work is to investigate the contribution to extrudate swell from these two aspects, namely as a result of velocity distribution and, by deduction, from viscosity variation.

MATHEMATICAL MODEL AND NUMERICAL METHOD

As mentioned above, a main aim of the current work is to estimate the contribution to extrudate swell from the velocity factor. And as will be discussed below, the contribution from the other factor, namely viscosity variation as a result of temperature change can then be deduced. Therefore, two problems need to be considered and their results compared.

In Problem One, a full extrusion situation is considered. Although results as regards extrudate swell of this problem have been reported elsewhere (Huynh, 1998b), because it forms the basis for comparison with Problem Two described below, this problem is described again. The die geometry considered in Problem One is in the form of a straight, circular tube on the outside, and a concentric cylindrical mandrel with a conical head facing the flow on the inside, thus forming a uniform annular gap between them before the die exit. The arrangement is shown diagrammatically in Fig. 1. The chosen geometry is believed to be representative enough of an extrusion process through annular dies; see, for example, Powell (1974), Morton-Jones (1989), Benbow and Bridgwater (1993) for some similar geometries.
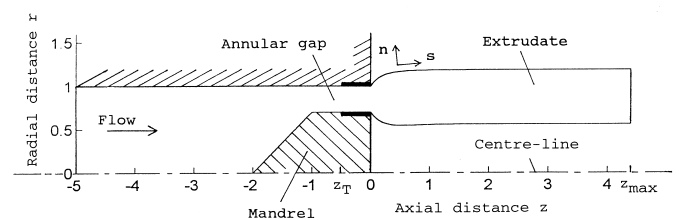

Figure 1. Model of the flow domain and die geometry for Problem One.

The mathematical model used is that for a steady, axi-symmetric, non-isothermal flow of incompressible, Newtonian fluids with free surfaces and without body forces. The governing equations are those of conservation of mass and momentum, and balance of energy. For ease of reference, a non-dimensionalisation scheme is also used and the non-dimensional parameters and variables are defined such that the form of the governing equations is unchanged (Huynh, 1998a). In the usual notation, these equations in cylindrical coordinates are (Bird et al., 1964)

Conservation of mass:

$$\frac{\partial u}{\partial r} + \frac{u}{r} + \frac{\partial w}{\partial z} = 0$$

Conservation of momentum:

$$\rho \left(u \frac{\partial u}{\partial r} + w \frac{\partial u}{\partial z} \right) = -\frac{\partial p}{\partial r} +$$

$$\mu \left(\frac{\partial^2 u}{\partial r^2} + \frac{\partial (u/r)}{\partial r} + \frac{\partial^2 u}{\partial z^2} \right)$$

$$\rho \left(u \frac{\partial w}{\partial r} + w \frac{\partial w}{\partial z} \right) = -\frac{\partial p}{\partial z} +$$

$$\mu \left(\frac{\partial^2 w}{\partial r^2} + \frac{1}{r} \frac{\partial w}{\partial r} + \frac{\partial^2 w}{\partial z^2} \right)$$

Balance of energy:

$$\rho c \left(u \frac{\partial T}{\partial r} + w \frac{\partial T}{\partial z} \right) =$$

$$k \left(\frac{\partial^2 T}{\partial r^2} + \frac{1}{r} \frac{\partial T}{\partial r} + \frac{\partial^2 T}{\partial z^2} \right) +$$

$$2\mu \left[\left(\frac{\partial u}{\partial r} \right)^2 + \left(\frac{u}{r} \right)^2 + \left(\frac{\partial w}{\partial z} \right)^2 + \frac{1}{2} \left(\frac{\partial u}{\partial z} + \frac{\partial w}{\partial r} \right)^2 \right]$$

where r, z are respectively the (non-dimensional) radial and axial co-ordinates, u and w the velocity components in the radial and axial direction respectively, p pressure, T temperature, and ρ, μ, c and k respectively the fluid density, viscosity, specific heat capacity and thermal conductivity.

Note that for a Newtonian fluid and in Cartesian component form, the stress t_{ij} is related to pressure and strain rates by

$$t_{ij} = -p \, \delta_{ij} + \mu \left(\frac{\partial v_i}{\partial x_j} + \frac{\partial v_j}{\partial x_i} \right)$$

where v_i is the velocity in the x_i direction, and δ_{ij} the Kronecker delta.

The coupling between the flow and temperature fields is via the fluid's temperature-dependent viscosity. Here μ is assumed to decrease exponentially with temperature according to the formula

$$\mu = \mu_o \, e^{-\alpha T}$$

where α is a non-dimensional exponential coefficient and μ_o a constant, here set equal to 1. Other fluid properties are assumed to be constant, and the following non-dimensional values are used: density $\rho = 1.67 \times 10^{-7}$; thermal conductivity $k = 0.190$; specific heat capacity $c = 7.19 \times 10^{7}$. It was shown (Huynh, 1998a) that when appropriate values are taken for the physical parameters like temperatures, mean flow velocity, tube radius, etc., then the above non-dimensional properties correspond approximately to those of low-density polyethylene under zero shear at about 150°C - 190°C temperature range.

Referring to Fig. 1, the following non-dimensional boundary conditions are used:

(a) At entrance to the flow domain ($z = -5$): parabolic velocity profile and uniform, zero temperature,

$$u = 0 \, , \; w = 2 \left(1 - r^2 \right) , \; T = 0$$

(b) The tube wall and mandrel wall, here together called the die walls, are divided into two sections.

(i) Section 1, between entrance to the flow domain ($z = -5$) and a location $z = z_T < 0$ in the annulus region upstream of the die exit: non-slip condition and zero temperature,

$$u = w = 0 \, , \; T = 0$$

(ii) Section 2, between the location $z = z_T$ and die exit ($z = 0$), shown as ■■■ in Fig. 1: non-slip condition and some imposed wall temperatures,

$$u = w = 0$$

$T = T_{in}$ on the inner (mandrel) wall, $T = T_{out}$ on the outer (tube) wall

(c) Along the centre-line ($r = 0$, $z \leq -2$): zero radial velocity and shear stress, and axis-of-symmetry condition for temperature,

$$u = 0 \, , \; t_{rz} = 0 \, , \; \partial T / \partial r = 0$$

(d) At the "far-downstream" section or exit of the flow domain ($z = z_{max}$ where z_{max} is sufficiently large so that there is no further change to the extrudate dimensions; here values of $z_{max} = 4$, 4.4 and 6 have been used): zero radial velocity and axial stress,

$$u = 0 \, , \; t_{zz} = 0$$

No thermal boundary condition is imposed on this end, thus the solution attempts to make $\partial T / \partial z = 0$ here. This is acceptable, as discussed in Phuoc and Tanner's (1980).

(e) On the free surfaces ($z > 0$) : zero stresses

$$t_{nn} = t_{ns} = 0$$

where n is the (non-dimensional) outward-pointing co-ordinate normal to the surfaces, and s is the co-ordinate along them. Also a convective cooling condition is imposed. Here, following Phuoc and Tanner (1980), this is

$$\frac{\partial T}{\partial n} = -0.72 \, T - 28.8$$

In Problem Two, the flow domain consists simply of the extrudate of Problem One, i.e. the part with $z \geq 0$. The viscosity's exponential coefficient α is set to zero, and thus

in effect making the problem isothermal as regards the flow field. The boundary conditions are as follows:

At inlet to the considered flow domain, i.e. along the section $z = 0$ which corresponds to the die exit in Problem One, the velocity results of Problem One are prescribed. Because $\alpha = 0$, temperature has no effects on the flow field, and any arbitrary set of temperature values can be used for thermal boundary conditions; here mostly $T = 0$ has been used.

On the rest of the boundary, i.e. on the free surfaces and at the "far-downstream" section (exit of the considered flow domain) the same boundary condition as for Problem One are prescribed; i.e. boundary conditions *(d)* and *(e)* above.

A finite element scheme based on the Galerkin discretisation procedure is used, solving numerically the governing equations simultaneously in their full, non-linear forms, together with boundary conditions, for the primary variables which consist of the two velocity components, pressure and temperature. A simple iterative scheme of successive substitution type (Picard method) is used for the solution of the resultant set of non-linear algebraic equations. The correct working of the resultant computer program used has been amply demonstrated before (Tanner et al., 1975; Phuoc and Tanner, 1980; Huynh, 1998a).

For Problem One, grid patterns of 11 quadrilateral elements in the radial direction by 81 elements in the axial direction (12×82 grid points) and 13 by 98 elements (14×99 grid points) are used. The adequacy of these patterns is ascertained by observing that solutions obtained from the 12×82 grid are very similar to those from the 14×99 grid for the many test cases where both grids are used. The grid patterns for Problem Two are simply those corresponding to the extrudate part of Problem One. Thus patterns of 12×48, 12×51 and 14×59 grid points have been used. Also, for all cases presented here, numerical convergence has been ensured to be excellent. (Figs 9 and 10 below show examples of the grid patterns that have resulted after convergence has occurred. The patterns are for the corresponding cases from the two problems).

In addition to the "grid convergence" tests mentioned above, another set of tests have also been performed to ensure the validity of the solutions obtained. In these tests, a modified, non-isothermal Problem Two is solved, whereby α *is now non-zero* and being the same as that of the corresponding cases of Problem One. At inlet to the flow domain, boundary conditions now include the temperature results at die exit from the corresponding cases of Problem One. Solutions from the two problems as regards extrudate parameters are then compared. The agreement has been satisfactory. For example, the results shown in Table 1 have been obtained at the "far-downstream" location ($z = 6$) for the case where $\alpha = 0.100$, and annular radius ratio $R_{inner\ wall} / R_{outer\ wall}$ of 0.7.

	from Problem One	from modified, non-isothermal Problem Two
Inner Radius	1.5505	1.5595
Outer Radius	1.9721	1.9838
Axial Velocity	0.673	0.664
Temperature on inner surface	− 10.62	− 10.71
Temperature on outer surface	− 10.96	− 11.05

Table 1. An example of extrudate's parameters obtained from solving corresponding cases of Problem One and the modified, non-isothermal Problem Two.

Computation is done on a *Sun Enterprise 3000* machine, running a UNIX operating system. Double precision (64 bits) is used throughout.

RESULTS AND DISCUSSION

Two annulus ratios $R_{inner\ wall} / R_{outer\ wall}$ of 0.7 and 0.9, as well as the degenerative situation of capillary extrusion when the mandrel core is absent are considered under a combination of different imposed wall temperatures. The combination results in a total of 13 "*case series*" for Problem Two as listed in Table 2. The solutions from these series will then be compared with the corresponding situations from Problem One, also listed in Table 2 and which have been reported by Huynh (1998b). Thus, in total, results from 26 *series* will be presented. Another parameter of interest would be a changing value of z_T (see Fig. 1) but presently only a value of $z_T = - 0.5$ is used. The series are also grouped into 3 groups according to the annular gap size. Within each series of Problem One, the fluid viscosity's exponential coefficient α is varied, allowing the Nahme-Griffith number Na to change as a primary changing parameter. The Nahme-Griffith number based on conditions at exit in Problem One is defined as

$$Na = \alpha\, W^2 \mu_o / k$$

where W is the mean velocity in the axial direction. The Péclet number at the exit, defined as

$$Pe = \rho\, c\, W\, (R_o - R_i) / k$$

is, however, constant within each series; here R stands for radius, and subscripts o and i indicate outer and inner radii respectively. It should be pointed out that Pe represents the ratio between convective and conductive heat transfers. On the other hand, since α^{-1} can be considered as a characteristic temperature change, Na provides a measure of the relative change in viscosity due to heat generation and thus determines the amount of coupling between the flow field and temperature field. For the cases of Problem One considered here, Na is related to α by the following relations

$$
\begin{aligned}
Na &= 20.20\ \alpha \quad \text{for group } \boldsymbol{B} \text{ (series } B, Bm, Bn, \text{ etc.)}\\
&= 145.6\ \alpha \quad \text{- - - - - - } \boldsymbol{D} \text{ (- - - } D, Dm, Dn, \text{ etc.)}\\
&= 5.26\ \alpha \quad \text{- - - - - - } \boldsymbol{O} \text{ (- - - } O, Om, On)
\end{aligned}
$$

Below, occasionally, we identify an individual case of a series by the series letter followed by the Na value. Also note that the matching cases from the two Problems are

distinguished by an extra *0* associated with Problem Two. Thus, for example *Bp2.02* indicates a case of series *Bp* from Problem One with the *Na* = 2.02 (α = 0.100), while the corresponding case from Problem Two (for which *Na* is always *zero*) is designated as *Bp02.02*.

The local Reynolds number based on a local length scale *L* and defined as $Re = \rho W L / \mu$ usually attains its maximum value near the die exit of Problem One as μ would be smallest in that region due to prolonged viscous heating in the annulus giving rise to a maximum temperature. In all cases, however, *Re* is very small. Using the annular gap size

Extrudate thickness swell ratio

$$s_t = [extrudate\ thickness - exit\ gap\ size] / exit\ gap\ size$$
$$= [(R_o - R_i)_{extrudate} - (R_o - R_i)_{exit}] / (R_o - R_i)_{exit}$$

Mean radius swell ratio

$$s_m = [(R_m)_{extrudate} - (R_m)_{exit}] / (R_m)_{exit}$$

where R_m is the mean radius given by $R_m = (R_o + R_i)/2$. Thus s_m provides a measure of the extrudate's radial deflection relative to the die exit location.

Group	Annular gap radii	Case series	T_{in}/T_{out} of Problem One	Grid pattern used (grid points) - Problem One	Grid pattern used (grid points) - Problem Two	Péclet number *Pe*
B	0.7 - 1 (Gap size 0.3)	B	0 / 0	14 × 99		37.1
		B0			14 × 59	
		Bm	− 16 / − 16	14 × 99		
		Bm0			14 × 59	
		Bn	+ 16 / + 16	12 × 82		
		Bn0			12 × 48	
		Bo	− 16 / + 16	12 × 82		
		Bo0			12 × 48	
		Bp	+ 16 / − 16	14 × 99		
		Bp0			14 × 59	
D	0.9 - 1 (Gap size 0.1)	D	0 / 0	14 × 99		33.2
		D0			14 × 59	
		Dm	− 16 / − 16	14 × 99		
		Dm0			14 × 59	
		Dn	+ 16 / + 16	12 × 82		
		Dn0			12 × 48	
		Do	− 16 / + 16	14 × 99		
		Do0			14 × 59	
		Dp	+ 16 / − 16	14 × 99		
		Dp0			14 × 59	
O	0 - 1 (no annulus: capillary extrusion)	O	− / 0	12 × 82		63.1
		O0			12 × 51	
		Om	− / − 16	12 × 82		
		Om0			12 × 51	
		On	− / + 16	12 × 82		
		On0			12 × 48	

Table 2. Cases considered.

for *L* and the minimum value attained near the die exit for μ, the maximum *Re* attained is about 1.3×10^{-4}.

Extrudate Swells

To characterise swelling in extrusion through annular dies, the following two swell ratios are used (subscripts *extrudate* and *exit* indicate the conditions at the "far-downstream" section of the extrudate and at the die exit, respectively):

In the following, *Na* refers to *Na* of Problem One, since for Problem Two *Na* is always zero. Also, as regards extrudate swell, values corresponding to *Na* = 0 will be used as reference ones. Furthermore, it should be mentioned that the extrudate's swelling behaviour resulting from Problem One has been discussed previously elsewhere (Huynh, 1998b). Here, attention will be given to results of Problem Two, but comparison will be made between the two Problems. Thus, for example, an s_m value obtained from the case *Bp02.02* of Problem Two would indicate a contribution from the velocity factor to the total value that has been obtained from the corresponding case *Bp2.02* of Problem One.

Figs 2 and 3 show some representative velocity profiles at die exit from Problem One that have been used as velocity boundary conditions at inlet (*z* = 0) to the flow domain in Problem Two. The figures also show the corresponding temperature profiles which have been used in the second set of validation tests mentioned above. Note that Fig. 2 shows a flattening of the *w* profile and a shifting of the *u* profile's peak value towards the die walls as their equal temperature increases. Fig. 3 on the other hand shows a shifting of the *w* profile and maximum *u* values towards the hot wall side. These behaviours are expected however, since a hot wall would reduce viscosity locally, and enhances the flow.

Variation of s_t with respect to Problem One's *Na* for the series of group *O* is shown in Fig. 4. Note that for this group, s_t and s_m are identical. By comparing the results between series *O* and *O0*, and between *Om* and *Om0*, it can be seen that velocity distribution contributes to a very small portion of extrudate swell when zero or negative temperatures are imposed on the die wall.

Now one important implication of the results of the second set of validation tests mentioned above is that, as regards extrudate swell, it can be solely determined by the distribution of velocity and temperature (hence viscosity) at die exit. This then means that viscosity change due to temperature is the principal cause of extrudate swell in circular capillary extrusion when zero or negative temperatures are imposed on the die wall. When the wall is heated, however, a comparison of results from series *On* and *On0* shows that the velocity factor can constitute a

substantial proportion of extrudate swell; here up to about 44% of the total.

Figs 5 and 6 show variation of s_t with respect to Problem One's Na for the series of groups $\boldsymbol{B}$ and $\boldsymbol{D}$ respectively. By comparing results from series B and $B0$, Bm and $Bm0$, Bn and $Bn0$, and similarly with the series of group $\boldsymbol{D}$, it can be seen that when both annulus walls have the same temperature, velocity factor constitutes a very small portion of the total thickness swell, with the exception of series Bn and $Bn0$ whereby this portion can be up to about 27 %. Note that with these two latter series a contraction in extrudate thickness occurs, using the s_t value at zero Na as reference. However, when temperatures of opposite signs are imposed on the annulus walls, contribution from the velocity factor to thickness swell becomes substantial. This can be seen in the comparison between series Bo and $Bo0$, Bp and $Bp0$, Do and $Do0$, and Dp and $Dp0$. Also, the proportion is higher in group $\boldsymbol{B}$, reaching, for example, to a maximum of about 27 % with series Bo and $Bo0$ at $Na = 1.01$.

One other interesting aspect is that with series $Bp0$ and $Dp0$ a suppression of thickness swell by the velocity distribution has occurred, against the large, positive trend of series Dp, and especially Bp at higher Na values. This thus indicates an even stronger influence of viscosity on thickness swell in these series.

Figs 7 and 8 show variation of s_m from the two Problems in terms of Na for groups B and D respectively. When both die walls have the same temperatures (series B and $B0$, Dm and $Dm0$, etc.), s_m in all cases is very small and thus both velocity and viscosity have very little influence on s_m.

However, when different temperatures are imposed on the die walls (series Bo and $Bo0$, Dp and $Dp0$, etc.), the velocity factor in general contributes to a substantial portion of the total s_m. Furthermore, this portion is larger when the cold wall is on the inside (series Bo and $Bo0$, Do and $Do0$). Also, in terms of magnitude, s_m from the series of group $\boldsymbol{B}$ is larger (relative to the reference values at $Na = 0$) than that from group $\boldsymbol{D}$; as regards Problem One the reason for this has been shown to be related to the higher Péclet number of group $\boldsymbol{B}$ (Huynh, 1999). The proportion of contribution to s_m from the velocity factor is, however, mostly minor (less than about 40 %), except for the corresponding series Bo and $Bo0$ where the ratio of s_m reaches about 57 %. The reason for this high ratio is believed to be mainly due to the levelling out of s_m of the Bo series at high Na, which is in turn due to the larger annular gap of group $\boldsymbol{B}$; essentially, the extrudate's inner radius has a lower limit of zero, and group $\boldsymbol{B}$ would reach its limit before that of group $\boldsymbol{D}$.

Finally, Figs 9 and 10 show an example of extrudate shape from corresponding cases of the two Problems, with the resulting grid patterns of the flow domains after convergence has occurred; the cases being $Bo2.02$ and $Bo02.02$ respectively.

CONCLUSIONS

In an effort to provide further understanding of the extrudate's swelling behaviour in non-isothermal extrusion, contribution to extrudate swell from the velocity factor has been investigated numerically. Contribution from the other factor due to variation in fluid viscosity as a result of temperature change can then be estimated by deduction. Annular and circular dies have been considered. It is found that contribution from the velocity factor to thickness swell and deflection of the extrudate depends significantly on thermal conditions of the die walls. With circular dies, this contribution is substantial only when the die walls are heated. With annular dies, the contribution is seen to vary with die gap size. However, when both walls are imposed with the same temperatures, this contribution remains mostly small, except for thickness swell in the case of larger die gap whose walls are heated. When different temperatures are imposed on the die walls such that one is heated while the other is cooled, the velocity factor can then contribute a substantial portion to the total swelling effect. In most cases, however, this portion is still minor, leaving viscosity change through temperature variation as the major cause of extrudate swell.

REFERENCES

AHN, Y.-C. and RYAN, M. E., 1992, Analysis of nonisothermal extrudate swell, *Chem. Eng. Comm.* **116**, 201-225

BIRD, R. B., W. E. STEWART and E. N. LIGHTFOOT, 1960, *Transport Phenomena*, John Wiley

BENBOW, J. and J. BRIDGWATER, 1993, *Paste Flow and Extrusion*, Oxford University Press

HUYNH, B. P., 1983, Some Finite Element Studies of Extrusion, *J. Non-Newtonian Fluid Mech.* **13**, 1-20

HUYNH, B. P., 1998a, A numerical investigation of non-isothermal extrusion through annular dies, *Int. J. Engng Sci.* **36**(2), 171-188

HUYNH, B. P., 1998b, A numerical investigation of non-isothermal extrusion through annular dies - Influence of wall temperatures on extrudate swell, *Heat Transfer 1998, Proc. 11th Int. Heat Transfer Conf.* **5**, 27-32, August 23-28, Kyongju, Korea

HUYNH, B. P., 1999, A numerical study of the influence of wall temperatures in extrusion through annular dies, *submitted*

KARAGIANNIS, A., A. N. HRYMAK and J. VLACHOPOULOS, 1989, Three-dimensional non-isothermal extrusion flows, *Rheologica Acta* **28**, 121-133

MITSOULIS, E., 1986, Extrudate swell of Newtonian fluids from annular dies, *AIChE J.* **32**(3), 497-500

MORTON-JONES, D. H., 1989, *Polymer Processing*, Chapman & Hall

PHUOC, H. B. and TANNER, R. I., 1980, Thermally-induced extrudate swell, *J. Fluid Mech.* **98**, 253-271

POWELL, P. C., 1974, Design of extruder dies using thermoplastics melt properties data, *Polym. Eng. Sci.* **14**, 298-307

SEO, Y., 1990, Nonisothermal annular die swelling analysis, *Polym. Eng. Sci.* **30**(4), 235-240

TANNER, R. I., R. E. NICKEL and R. W. BILGER, 1975, Finite element methods for the solution of some incompressible non-Newtonian fluid mechanics problems with free surfaces, *Comput. Methods Appl. Mech. Eng.* **6**, 155-174

TANNER, R. I., 1980, A new inelastic theory of extrudate swell, *J. Non-Newtonian Fluid Mech.* **6**, 289-302

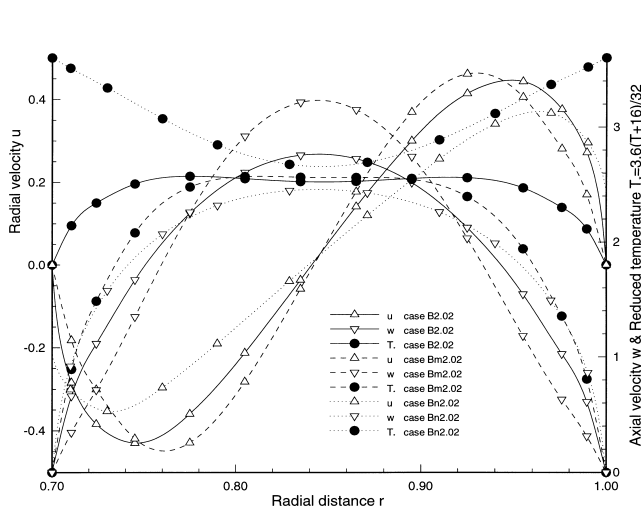VLACHOPOULOS, J., 1981, Extrudate swell in polymers, *Rev. Deform. Beh. Materials* **3**, 219-248

Figure 4. Variation of s_t with respect to Problem One's *Na* for the series of group $\boldsymbol{O}$.

Figure 2. An example of velocity profiles at die exit from the solution of Problem One and used as boundary conditions at inlet to the flow domain in Problem Two. Here the die walls have the same temperature. The temperature profiles are also shown.
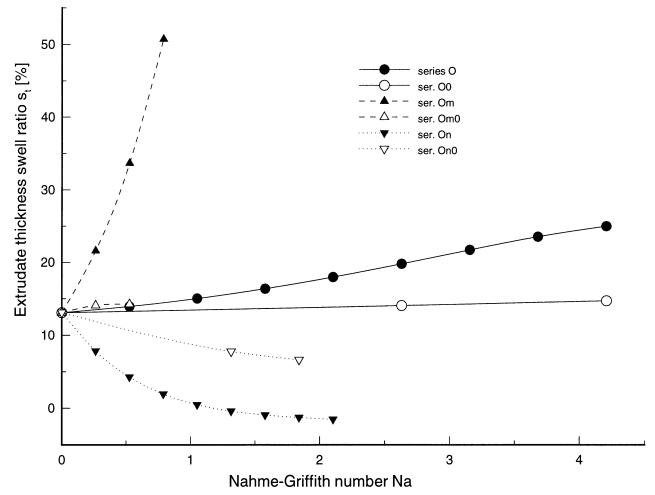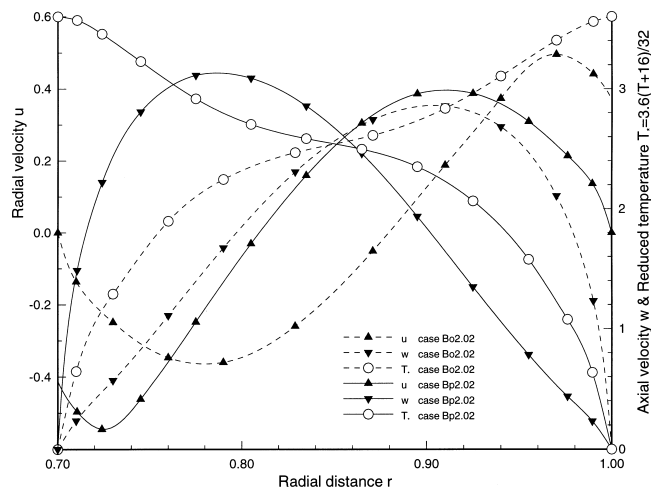

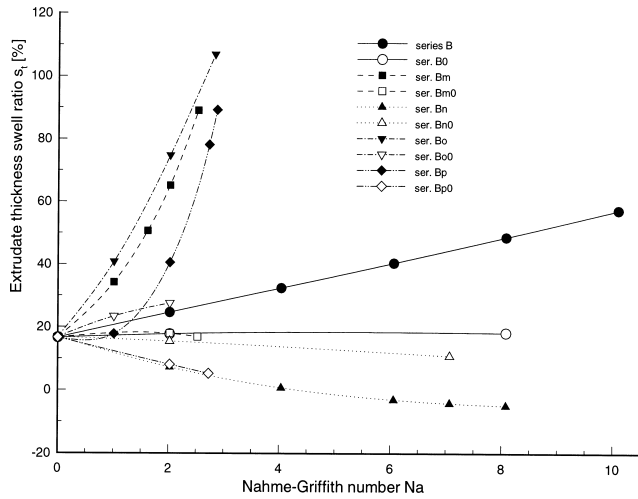**Figure 3**. Similar to Figure 2, but here the die walls are prescribed with temperatures of the opposite signs.

Figure 5. Variation of s_t with respect to Problem One's *Na* for the series of group ***B***.
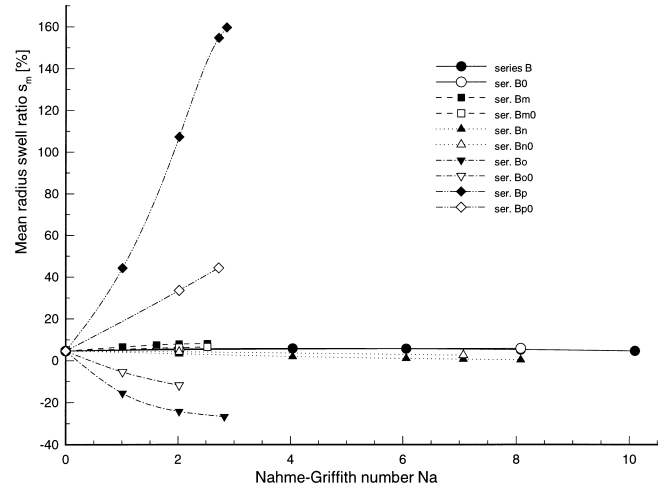
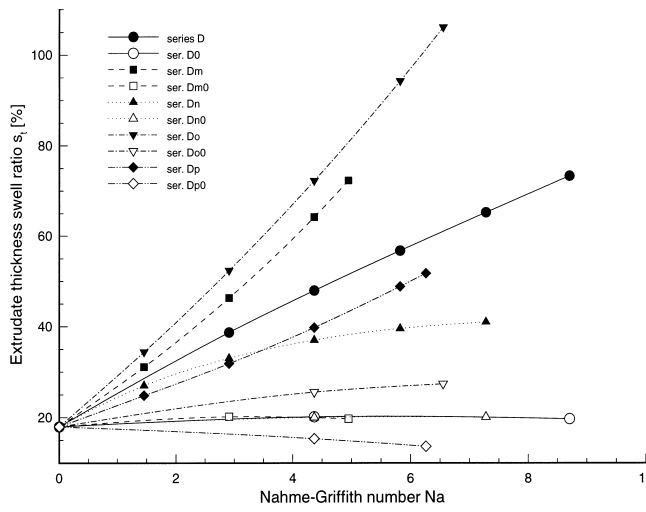**Figure 7**. Variation of s_m with respect to Problem One's *Na* for the series of group ***B***.

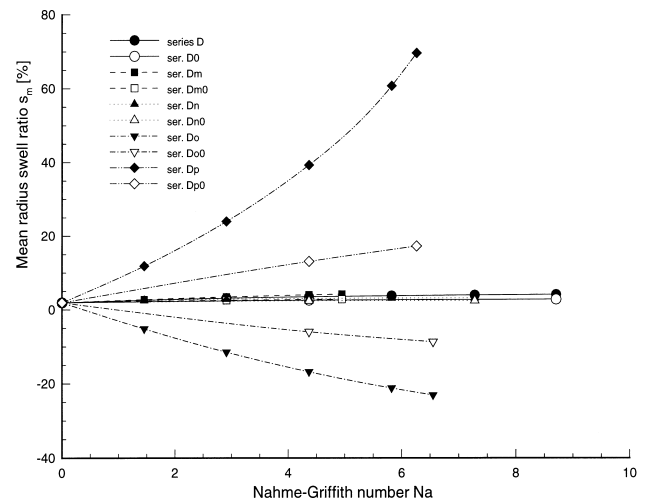**Figure 6**. Variation of s_t with respect to Problem One's *Na* for the series of group ***D***.

Figure 8. Variation of s_m with respect to Problem One's *Na* for the series of group ***D***.
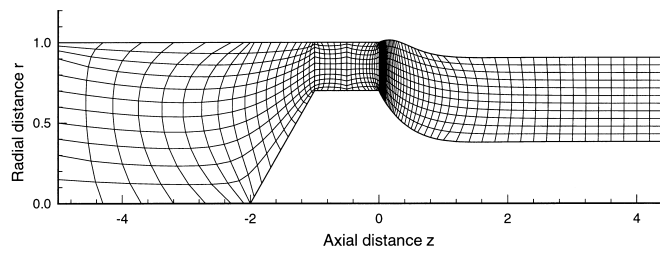
Figure 9. An example case of Problem One showing extrudate shape and the resulting flow domain's grid pattern after convergence has occurred. The case is *Bo2.02* of series *Bo* with *Na = 2.02*.
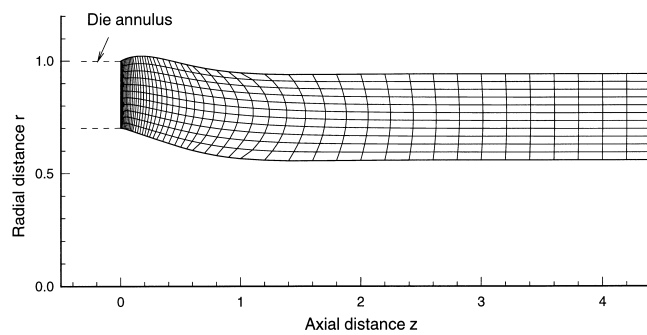

Figure 10. An example case of Problem Two, showing the shape of the flow domain (extrudate only) and the resulting grid pattern after convergence has occurred. The case is *Bo02.02* of series *Bo0*, corresponding to the case *Bo2.02* shown in Figure 9.